

Serveur Académique Lausannois SERVAL serval.unil.ch

Author Manuscript

Faculty of Biology and Medicine Publication

This paper has been peer-reviewed but does not include the final publisher proof-corrections or journal pagination.

Published in final edited form as:

Title: Subconjunctival injection of XG-102, a c-Jun N-terminal kinase inhibitor peptide, in the treatment of endotoxin-induced uveitis in rats.

Authors: El Zaoui I, Touchard E, Berdugo M, Abadie C, Kowalczyk L, Deloche C, Zhao M, Naud MC, Combette JM, Behar-Cohen F

Journal: Journal of ocular pharmacology and therapeutics : the official journal of the Association for Ocular Pharmacology and Therapeutics

Year: 2015 Feb

Volume: 31

Issue: 1

Pages: 17-24

DOI: 10.1089/jop.2014.0019

Title:

Subconjunctival injection of XG-102, a c-Jun N-terminal kinase inhibitor peptide, in the treatment of endotoxin-induced uveitis in rats.

Authors:

Ikram El-zaoui^{1,2,3}, Elodie Touchard^{1,2,3}, Marianne Berdugo^{1,2,3}, Claire Abadie⁴, Laura Kowalczuk^{1,2,3}, Catherine Deloche⁴, Min Zhao^{1,2,3}, Marie-Christine Naud^{1,2,3}, Jean-Marc Combette⁴, Francine Behar-Cohen^{1,2,3,5}.

¹INSERM UMRS 872, Team 17 Physiopathology of Ocular Diseases: Therapeutic Innovations, Paris, France.

²Pierre et Marie Curie University, Centre de Recherches des Cordeliers, Paris, France.

³Paris Descartes university, UMRS 872, Paris, France.

⁴Solid Drug Development S.A., Geneva, Switzerland.

⁵Department of Ophthalmology of University of Lausanne, Jules Gonin Hospital, Fondation asile des Aveugles, Switzerland

***Correspondence to:** Correspondence should be addressed to Francine Behar-Cohen

Address: Centre de Recherches Biomédicales des Cordeliers, UMR S 872, Team 17 « Physiopathology of ocular diseases: Therapeutic innovations », Pierre et Marie Curie University, Paris Descartes University; 15 rue de l'école de médecine; F-75006 Paris, France.

Tel: +33 1 44 27 81 69. Fax: +33 1 44 27 81 12. Emailaddress: francine.behar@gmail.com

ABSTRACT

[Aim] XG-102 is a TAT-coupled dextrogyre peptide inhibiting the c-Jun N-terminal kinase. With a molecular weight of 5000 and a resistance to proteases, we hypothesized that XG-102 could be used locally as a long acting anti-inflammatory agent. We tested different routes of administration and doses in rat endotoxin-induced uveitis (EIU).

[Methods] XG-102 was administered at the time of LPS challenge either by intravenous (IV; 3.2, 35 or 355 $\mu\text{g}/\text{injection}$), intravitreal (IVT; 0.08, 0.2 or 2.2 $\mu\text{g}/\text{eye}$) or sub-conjunctival (SCJ; 0.2, 1.8 or 2.2 $\mu\text{g}/\text{eye}$) injections. Controls received either the vehicle or Dexamethasone phosphate injections. Efficacy was assessed by clinical scoring, infiltrating cells count, and expression of inflammatory mediators (iNOS, CINC-1). Effect of XG-102 on phosphorylated c-Jun was evaluated on Western-bolt.

[Results] XG-102 clinically demonstrated a dose-dependent anti-inflammatory effect in EIU after IV and SCJ administrations. The respective doses of 35 μg and 1.8 μg were efficient as compared with the vehicle-injected controls, but only the highest doses, respectively 355 μg and 2.2 μg , were as efficient as Dexamethasone. IVT injections of XG-102 at all tested doses was as efficient as dexamethasone. The clinical effect of XG-102 correlated well with reduction of c-Jun N-terminal kinase activity; infiltration of cells and iNOS and CINC-1 expression.

[Conclusion] Local administration of XG-102 can be used as efficiently as systemic route for the treatment of ocular inflammation. results confirm that XG-102 have potential for treating intra-ocular inflammation.

Introduction

Intraocular inflammation has an annual incidence of 52 cases per 100,000, resulting in a prevalence of about 115 per 100,000 [1]. Acute anterior uveitis (AAU) is by far the most common form of uveitis representing around 80% of the cases. Its recurrent nature may result in secondary complications such as cataract, cystoid macular edema, glaucoma and, ultimately, destruction of the intraocular tissues and blindness [Error! Reference source not found., Error! Reference source not found.]. Current treatments for uveitis include corticosteroids [Error! Reference source not found.], immunosuppressive agents as tumor-necrosis factor-alpha (TNF- α) inhibitors and cyclosporine in corticosteroid-resistant cases, or chemotherapeutic agents as cyclophosphamide in severe uveitis. These pharmacological agents are delivered through topical and peri-ocular routes in AAU that are not associated with systemic diseases. Corticosteroids agents show clear clinical benefits but their chronic use is associated with many sight-threatening side effects, such as glaucoma, cataract, whilst systemic immunosuppressive agents are associated with general side effects [1, Error! Reference source not found.]. Given these restrictions, there is an obvious demand for the development of new local therapeutic strategies [Error! Reference source not found.].

Current clinical trials concern the development of sustained-release delivery system like corticosteroid intravitreal implants [Error! Reference source not found.], as well as new immunosuppressive drugs, as anti-pro-inflammatory cytokines: new anti-TNF- α agents, interleukin (IL) receptors as IL-6R and IL-1R, interferon-gamma (IFN- γ) antagonists...[Error! Reference source not found., clinicaltrials.gov]. Many of the gene products involved in the inflammatory response are regulated by the transcription factor activator protein-1 (AP-1) and the c-Jun NH₂-terminal kinase (JNK) pathways: TNF- α , IFN- γ , IL-2, membrane cofactor protein-1 (MCP-1), macrophage in-

1
2
3
4
5
6
7
8
9
10
11
12
13
14
15
16
17
18
19
20
21
22
23
24
25
26
27
28
29
30
31
32
33
34
35
36
37
38
39
40
41
42
43
44
45
46
47
48
49
50
51
52
53
54
55
56
57
58
59
60

flammatory protein-1 alpha (MIP-1 α), cyclooxygenase-2 (COX-2), inducible nitric oxide synthase (iNOS)...

Among all the anti-inflammatory strategies in development, JNK inhibitors have been shown effective in various models of inflammation [Error! Reference source not found., Error! Reference source not found.] and could therefore be an interesting alternative to corticosteroid treatments in AAU. XG-102 is a TAT-coupled dextrogyre peptide which selectively inhibits the c-Jun N-terminal kinase *in vitro*. This peptide contains a 20-amino acid sequence of the JNK binding domain of islet-brain-1 (IB-1)/JNK-interacting protein-1 (JIP-1), a scaffold protein, combined to a 10-amino acid TAT sequence of the HIV TAT protein, allowing its intracellular penetration. The D-retro-inverso peptide - the reversed sequence of the D-amino acid form - retains the capacity of JNK inhibition and translocation, but has an extended activity due to its resistance to degradation by proteases [Error! Reference source not found.].

In a previous study, we brought the proof of principle that XG-102, administered either *via* intravitreal (IVT) or intravenous (IV) injections, efficiently inhibited intraocular inflammation in a rat model of endotoxin-induced uveitis (EIU) [Error! Reference source not found.]. In the prospect of a clinical trial, we evaluate herein different doses and routes and compare them to sub-conjunctival (SCJ) injections.

Material and Methods

Animals

Seven-week-old female Lewis rats (Elevage Janvier, Le Genest Saint Isle, France), weighing around 175 g, were used for experiments. All animals were treated according to the European

1 Convention and to the Association for Research in Vision and Ophthalmology (ARVO) State-
2 ment for the Use of Animals in Ophthalmic and Vision Research (French decree No.2001-486,
3
4 dated June 06, 2001). Rats were anesthetized with intramuscular injection of ketamine (Ketamine
5
6 Virbac[®], 88 mg/kg; Virbac, France) and chlorpromazine (Largactil[®], 0.6 mg/kg; Sanofi-Aventis,
7
8 Paris, France) before IV or ocular injections. Rats were sacrificed by a lethal dose of pentobarbi-
9
10 tal.
11
12

13 **Endotoxin-Induced Uveitis (EIU) induction and experimental design**

14
15 EIU is a model of acute and predominately anterior uveitis in rats [13]. Eighty two female Lewis
16
17 rats were randomly divided into fifteen groups of three to nine animals each. EIU was induced by
18
19 a single footpad injection of 100 μ L sterile pyrogen-free saline containing 200 μ g of lipo-
20
21 polysaccharide (from *Salmonella typhimurium*, Sigma-Aldrich, France). Animals were treated
22
23 with XG-102 immediately before EIU induction by IV injection (100 μ L), or by local (SCJ or
24
25 IVT) injections in the right eye (5 μ L). Contralateral left eyes were not treated. XG-102-treated
26
27 rats were compared with control uveitic rats injected with the vehicle (NaCl 0.9%) or with Dex-
28
29 amethasone phosphate that was used as positive control for anti-inflammatory activity on EIU.
30
31 Clinical ocular inflammation was scored 24 hours after EIU induction. At this time-point, retinal
32
33 pigment epithelium (RPE)-choroid-sclera complexes and neuroretinas were carefully dissected
34
35 from the enucleated eyes, snap frozen, and stored at -80°C until use, respectively, for the analysis
36
37 of c-Jun phosphorylation state by Western blot and for evaluation of inflammatory mediators
38
39 (iNOS and cytokine-induced neutrophil chemoattractant-1 (CINC-1)) expression by RT-PCR.
40
41 Tissues were collected from eyes treated with XG-102, with the vehicle and non injected eyes.
42
43
44
45
46
47
48
49
50
51 Three eyes collected from these groups were kept to evaluate inflammatory cell infiltration in
52
53 ocular tissues.
54

55 **Solutions and Injections**

1
2
3 XG-102 peptide was produced and purified by Polypeptide Laboratories (Strasbourg,
4
5 France). Once lyophilized; XG-102 powder was dissolved in the vehicle (NaCl 0.9%, Versol;
6
7 Aguetant, Lyon, France) at the concentration of 5 mg/mL under sterile conditions, and stored at -
8
9 80°C until use. For each experiment, XG-102 solutions were prepared extemporaneously at the
10
11 required concentration in the vehicle. A fraction of each diluted solution was stored at -80°C until
12
13 its assay by HPLC. A commercial solution of Dexamethasone phosphate at 4 mg/mL (Soludeca-
14
15 dron; Laboratoire Roussel, Paris, France) was used as positive control.

16
17
18
19
20 In our previous study, the anti-inflammatory effect of XG-102 in EIU was demonstrated with IV
21
22 dose of 20 µg/kg (3.5 µg/rat weighting 175 mg) and IVT dose of 0.2 µg/eye [12]. Based on these
23
24 results, three doses were chosen per route of administration. Three solutions were prepared at 32,
2
26
27 350 and 3550 µg/mL for IV injections. For the local treatments, three dilutions per type of injec-
28
29 tions were prepared: XG-102 solutions at 17.43 and 430 µg/mL for IVT injections and solutions
30
31 at 30, 360 and 4400 µg/mL for SCJ injections.

32
33 For the systemic treatment evaluation, 100 µL of vehicle, Dexamethasone phosphate (400
34
35 µg/injection) or XG-102 (3.2, 35 or 355 µg/injection) were injected in the tail vein with a 25-
36
37 gauge needle connected to a 1 mL syringe (Becton Dickinson, Le Pont de Claix, France). For the
38
39 local delivery study, 5 µL of vehicle Dexamethasone phosphate (20 µg/eye) or XG-102 solutions
40
41 were injected in the right eye using a 30-gauge disposable needle (BD-microfine syringes; nm
42
43 Medical, Asnières, Paris, France). In the XG-102-treated groups, right eyes received 0.08, 0.2 or
44
45 2.2 µg of XG-102 through IVT injection, and 0.2, 1.8 or 22 µg through SCJ injection.

50 51 **Clinical assessment of EIU**

52
53 Clinical examinations were performed by slit lamp microscopy 24 hours after EIU induction. The
54
55 severity of uveitis was scored, in a masked manner, on a scale from 0 to 5 for each eye, as de-
56
57 scribed previously [15] grade 0, no inflammation; grade 1, minimal iris and conjunctival vasodi-
58
59 scribed previously [15] grade 0, no inflammation; grade 1, minimal iris and conjunctival vasodi-
60

1
2
3 lation but without the observation of flare or cells in the anterior chamber; grade 2, moderate iris
4
5
6 and conjunctival vessel dilation but without evident flare or cells in the anterior chamber; grade
7
8 3, intense iris vessels dilation, flare, and fewer than 10 cells per slit lamp field in the anterior
9
10 chamber; grade 4, more severe clinical signs than grade 3, with cells in the anterior chamber, with
11
12 or without the formation of hypopion; grade 5, intense inflammatory reaction, fibrin formation in
13
14 the anterior chamber, and total seclusion of the pupil.
15
16
17
18
19

20 **Western Blot analysis of the phosphorylated form of c-Jun (phospho c-Jun)**

21
22 RPE-choroid-sclera complexes were snap frozen immediately after dissection and stored at -80°C
23
24 until use. Tissues were homogenized in 500 µL of lysis buffer, consisting in MOPS SDS Running
2
26 Buffer (Invitrogen, Cergy Pontoise, France) supplemented with a cocktail of protease (Roche
27
28 Diagnostics, Meylan, France) and phosphatase (Sigma-Aldrich, St-Quentin Fallavier, France)
29
30 inhibitors. After heating for 5 min at 100°C, equal amounts of proteins were separated by elec-
31
32 trophoresis in a NuPAGE 4-12% Bis-Tris gel (Invitrogen) using MOPS SDS Running Buffer.
33
34 The bands obtained were then electroblotted onto a nitrocellulose membrane (Schleicher &
35
36 Schuell BioScience, Dassel, Germany). Blots were sequentially incubated with a rabbit anti-
37
38 Phospho-c-Jun (Ser 63) primary antibody and an anti-rabbit IgG horseradish peroxidase (HRP)-
39
40 linked secondary antibody according to the manufacturer's instruction (Cell Signaling Technolo-
41
42 gy, Ozyme, St Quentin en Yvelines, France). Bands were visualized using the ECL Western Blot-
43
44 ting Detection Reagents Kit (Amersham Biosciences, Orsay, France). Blots were then dehybrid-
45
46 ized and rehybridized successively with a mouse monoclonal anti α -tubulin primary antibody
47
48 (1:400; Serotec, Düsseldorf, Germany) and a HRP conjugated goat anti-mouse IgG secondary
49
50 antibody (1:5000; Santa Cruz Biotechnology, Tebu-bio, Le Perray en Yvelines, France). The
51
52
53
54
55
56
57
58
59
60

1
2
3 relative band intensity for phospho c-Jun was calculated in comparison to that for α -tubulin after
4
5
6 densitometry analysis (on ImageJ software).
7

8 **Evaluation of inflammatory cells infiltration using immuno-histochemistry**

9
10 For immunohistochemical analysis, eyeballs were enucleated, fixed for 1 hour at room tempera-
11
12 ture in phosphate-buffered saline (PBS) containing 4% paraformaldehyde and rinsed overnight in
13
14 PBS. After careful orientation, samples were embedded in optimal cutting temperature compound
15
16 (Tissue-Tek; Sakura Finetek, Zoeterwoude, The Netherlands) and stored at -80°C. Frozen 10- μ m
17
18 sections were collected on Superfrost slides (Gerhard Menzel, Braunschweig, Germany) using a
19
20 cryostat (CM 3050S; Leica, Rueil-Malmaison, France). The frozen 10- μ m sections collected at
21
22 the optic nerve level were stained 5 min with 4', 6 diamidino-2-phenylindole solution (DAPI,
23
24 1:5000; Sigma-Aldrich), mounted in PBS:Glycerol (1:1) and examined with a fluorescence mi-
25
26 croscope Olympus BX51 (Rungis, France) coupled with a digital camera Olympus DP70. Poly-
27
28 morphonuclear (PMN) cells, identified by the shape of their nuclei stained with DAPI, were
29
30 quantified on three different frozenslides per eye (n=3 eyes per group). Results were expressed as
31
32 mean \pm SEM.
33
34
35
36
37
38
39
40

41 **Evaluation of inflammatory mediators expression (iNOS, CINC-1) using RT PCR**

42
43 Selected doses of XG-102 were used to evaluate the expression of iNOS mRNA (3.2 and 35 μ g for IV
44
45 injection, 0.2 and 2.2 μ g for IVT and 1.8 μ g for SCJ injection) and CINC-1 mRNA in eyes (35 μ g for IV
46
47 injection, 0.2 μ g for IVT and 1.8 μ g for SCJ injection).
48

49
50 Total RNA was extracted from the neuroretinas stored at -80°C according to the manufacturer's
51
52 instructions (RNeasy minikit, Qiagen, France). For each sample, 1 μ g total RNA was readjusted
53
54 according to the RNA optic density at 260 nm and transcribed in a total volume of 20 μ L using
55
56
57
58
59
60

1
2
3 Superscript II Reverse Transcriptase (Invitrogen, France) following the manufacturer's instruc-
4
5 tions.

6
7
8 Glyceraldehyde 3-phosphate dehydrogenase (GAPDH), iNOS and CINC-1 cDNA were amplified
9
10 in a total volume of 25 μ L containing 2 μ L of first-strand reaction product, 0.4 μ M of each primer
11
12 (sense and antisense), 0.4 μ M dNTP Mix, 1.5 mM MgCl₂, 1X PCR buffer and 2.5 U Taq DNA
13
14 polymerase (Invitrogen, France). Primers specific for GAPDH (sense: 5'-
15
16 ATGCCCCCATGTTTGTGATG-3'; antisense: 5'-ATGGCATGGACTGTGGTCAT-3'), primers
17
18 specific for CINC-1 (sense: 5'-GGGTGTCCCCAAGTAATGGA-3'; anti-sense: 5'-
19
20 CAGAAGCCAGCGTTCACCA-3') and primers specific for iNOS (sense: 5'-
21
22 TTTCTCTTCAAAGTCAAATCCTACCA-3'; antisense: 5'-
23
24 TGTGTCTGCAGATGTGCTGAAAC-3') were obtained from Invitrogen. After an initial dena-
25
26 turation (1 min at 94°C), 34 to 37 PCR cycles of denaturation (30 s at 94°C), annealing (1 min at
27
28 58°C for GAPDH, at 60°C for CINC and at 52°C for iNOS) and elongation (1-2 min at 72°C)
29
30 were performed on a Crocodile III (Appligene-Oncor). The final cycle was completed by 5 min
31
32 of elongation at 72°C. PCR fragments (162 bp for GAPDH, 53 bp for CINC and 657 bp for iN-
33
34 OS) were analyzed by 2.5% agarose gel electrophoresis and visualized by ethidium bromide
35
36 staining under ultraviolet light. The relative bands intensity for CINC-1 and iNOS were calculat-
37
38 ed in comparison to that for GAPDH after densitometry analysis using ImageJ software.
39
40
41
42
43
44

45 46 47 48 **Statistical analysis**

49
50
51 Numerical results were expressed as mean \pm standard error mean (SEM) and compared using the
52
53 nonparametric Mann-Whitney U-test. $P < 0.05$ was considered statistically significant.
54
55
56
57
58
59
60

Results

XG-102 clinical effect on EIU using different routes of administration

Clinical scores were evaluated 24 hours after EIU induction which is the peak of inflammation in this model. Using either IV or SCJ injections (Fig 1 A and C), a dose-response effect was observed: the lowest doses (3.2 μg for IV and 0.2 μg for SCJ) were not efficient; increasing the dose induced increased anti-inflammatory effects. At the highest tested doses (355 μg IV, 2.2 μg IVT and 22 μg SCJ), the anti-inflammatory effects of XG-102 observed were better or equivalent to Dexamethasone phosphate, used as a positive control. The highest SCJ dose (22 μg) also significantly reduced inflammation in the contra lateral uninjected eye, suggesting a systemic passage of XG-102 at high dose. Using IVT injections, all tested doses significantly reduced intraocular inflammation with the same efficacy as Dexamethasone phosphate but with a reverse dose-response effect: the higher the dose, the less efficient is the drug (Fig 1B).

Effect of XG-102 on in vivo JNK phosphorylation

Western-blot analysis of the RPE-choroid-sclera complex collected at the peak of the disease demonstrated a reduced phosphorylation of c-Jun on Ser63 residue, using IV, SCJ and IVT (Fig 2). The densitometry analysis of Western blot showed a decrease in State of c-Jun phosphorylation in the samples either after 35 μg -XG-102 IV injection (0.284 vs 2.075 in vehicle IV; Fig 2A) or 1.8 μg -XG-102 SCJ injection (0.222 vs 1.436 in vehicle SCJ; Fig 2C). In the same manner, a reduction of c-Jun phosphorylation was observed in RPE-choroid-sclera complex after 0.2 μg -XG-102 IVT injection (0.205 vs 1.086 in vehicle IVT; Fig 2B).

Effect of XG-102 on ocular cell infiltration

Identified by the shape of their nuclei, stained with DAPI, polymorphonuclear cells (PMN) cells were quantified on histological sections of the ocular tissues. One day after 35 μ g-XG-102 IV delivery, the PMN cells infiltration decreased by 38% compared with vehicle IV injection (342 ± 50 vs 552 ± 151 , Fig 3A). Using IVT, 0.2 μ g-XG-102 delivery decreased by 48% the number of infiltrating cells as compared with the vehicle-injected eyes (97 ± 38 vs 186 ± 65 , Fig 3B). XG-102 SCJ administration decreased by 57% the PMN infiltration in the eyes treated with 1.8 μ g XG-102 as compared with the vehicle delivery (177 ± 41 vs 415 ± 87 , Fig 3C).

Expression of pro-inflammatory mediators

XG-102 reduced iNOS expression in ocular tissues whatever the route of administration.

In comparison with the vehicle-injected eyes, IV injections of 35 μ g XG-102 led to the downregulation of iNOS mRNA from 1.067 ± 0.037 to 0.390 ± 0.218 (-64%, Fig 4A). In IVT injected eyes with 0.2 μ g of XG-102, a 98% reduction in iNOS expression was observed (from 1.040 ± 0.001 to 0.02 ± 0.03 , Fig 4B) and 92% with 2.2 μ g XG-102 (from 1.04 ± 0.001 to 0.086 ± 0.06). Using SCJ delivery injection, iNOS expression decreased significantly by 86% in the right eyes treated with 1.8 μ g XG-102 as compared with the vehicle delivery (from 1.067 ± 0.037 to 0.100 ± 0.065 ; Fig 4C).

In order to confirm the reduced recruitment of inflammatory cells after XG-102 treatment, the expression of CINC-1, a mediator of neutrophil infiltration in the inflammatory sites, was evaluated in retinal cells at the mRNA level. As compared with the control group, the IV injection of 35 μ g of XG-102 reduced the CINC-1 expression from 0.382 ± 0.035 to 0.205 ± 0.063 (Fig 5A). The decrease of CINC-1 mRNA was also observed after IVT injection of 0.2 μ g of XG-102, from 0.584 ± 0.150 to 0.202 ± 0.063 as compared with the vehicle-injected eyes (Fig 5B). The SCJ

1
2
3 injection of 1.8 μg of XG-102 led to a down-regulation of CINC-1, from 1.05 ± 0.43 to $0.18 \pm$
4
5
6 0.03 as compared with the vehicle. However, in uninjected eyes no diminution of CINC-1 ex-
7
8 pression was observed after SCJ administration of 1.8 μg -XG-102 (Fig 5C). These results go
9
10 hand in hand with the decrease in PMNs infiltration in the eyes treated with: 35 μg -XG-102 IV,
11
12 0.2 μg -XG-102 IVT and 1.8 μg -XG-102 SCJ injections (Fig 3).
13
14
15
16
17
18

19 Discussion

20
21 The JNK pathway is activated in inflammatory reactions in various tissues of the body, particu-
22
23 larly the central nervous and the digestive systems [16,17]. Its specific inhibition by XG-102
24
25 blocks the phosphorylation of its nuclear target, c-Jun, which prevents the transcription of pro-
26
27 inflammatory cytokines/chemokines and the activation of the intracellular processes with harmful
28
29 results, such as cellular death by apoptosis [12, 18, 19]. In this study, we demonstrated that XG-
30
31 102 exerts anti-inflammatory effects on EIU using IV and IVT, as already shown in our previous
32
33 study [12], but also using SCJ injections. XG-102 is efficient at low-doses; since the 0.08 μg dose
34
35 directly injected into the vitreous was already efficient and increasing the dose did not increase
36
37 the effect. The anti-inflammatory activity was confirmed by reduced cell infiltration in ocular
38
39 tissues and decreased expression of iNOS and CINC-1 using specific dose for each tested route of
40
41 administration. Importantly, the anti-inflammatory effect correlated with the decreased phosphor-
42
43 ylation of JNK, demonstrating the specific mechanism of action of this drug.
44
45
46
47
48

49
50 For clinical used, SCJ injection of a D-peptide is particularly interesting. This route of admin-
51
52 istration is minimally invasive, with no risk of possible infection associated with IVT injections.
53
54
55 Moreover, XG-102 has a long half-life in vivo due to its resistance from proteases limiting the
56
57 need for re-injections [20]. SCJ of 1.8 μg was the lowest dose efficient clinically and biologically.
58
59
60

1
2
3 At 22 μg , the uninjected contralateral eye also showed reduced inflammation, suggesting a sys-
4
5
6 temic diffusion of XG-102 after SCJ in the treated eye. However, at a lower dose of 1.8 μg , no
7
8 effect was observed on the contralateral eye, suggesting a direct transscleral passage of XG-102
9
10 after SCJ without systemic diffusion. XG-102 is a small peptide with a molecular weight of
11
12 around 2.2 kDa adapted for transscleral diffusion. Indeed, previous works have shown that hy-
13
14 drophilic molecules up to 150 kDa were able to cross the sclera, the scleral permeability being
15
16 inversely proportional to the molecular weight [21]. Whether direct trans-corneal penetration of
17
18 XG-102 is occurring remains to be demonstrated. Sub-conjunctival injections are rarely used and
19
20 no drug is approved for such injections. However, studies comparing the ocular media levels of
21
22 Dexamethasone phosphate after oral administration, latero bulbar or sub-conjunctival injections
23
24 in humans, found that the highest concentrations in aqueous and vitreous humors were achieved
25
26 after SCJ injections.[22,23,24].
27
28
29

30
31
32 This is to our knowledge the first study evaluating the effect of sub-conjunctival injection of a
33
34 peptide for the treatment of uveitis. We have performed a first phase IIa clinical trial (EudraCT
35
36 Number: 2012-001510-14) to evaluate the safety and tolerance of XG-102 injected sub-
37
38
39 conjunctivally in patients with post-operative inflammation.
40

41
42 XG-102 injected either sub-conjunctivally or directly in the eye could be used in many ocular
43
44 diseases, associated with intraocular inflammation and/ or excitotoxicity.
45
46
47
48
49
50
51
52
53
54
55
56
57
58
59
60

References

1. De Smet MD, Taylor SR, Bodaghi B, Miserocchi E, Murray PI, Pleyer U, Zierhut M, Barisani-Asenbauer T, LeHoang P, Lightman S. Understanding uveitis. The impact of research on visual outcomes. *ProgRetin Eye Res* 2011Nov; 30 (6):452-470.
2. Mercieca K, Jones NP. Treatment of acute anterior uveitis in the community, as seen in an emergency eye centre. A lesson for the general practitioner?. *European Journal of General Practice* 2012 Mar; 18(1):26-9.
3. Medeiros R, Rodrigues GB, Figueiredo CP, Rodrigues EB, Grumman A Jr, Menezes-de-Lima O Jr, Passos GF, Calixto JB. Molecular mechanisms of topical anti-inflammatory effects of lipoxin A(4) in endotoxin-induced uveitis. *Mol Pharmacol* 2008 Jul; 74:154-161.
4. Taylor SR, Isa H, Joshi L, Lightman S. New developments in corticosteroid therapy for uveitis. *Ophthalmologica* 2010; 224(1):46-53.
5. Agrawal RV, Murthy S, Sangwan V, Biswas J. Current approach in diagnosis and management of anterior uveitis. *Indian J Ophthalmol* 2010; 58(1):11-19.
6. Abad S, Sève P, Dhote R, Brézin AP. Uvéites et médecine interne. Stratégies diagnostique et thérapeutique. *La Revue de médecine interne* 2009 Jun; 30(6):492–500.
7. De Smet MD. Corticosteroid intravitreal implants. *Dev Ophthalmol* 2012; 51:122-133.
8. Tsai ML, Horng CT, Chen SL, Xiao X, Wang CH, Tsao YP. Suppression of experimental uveitis by a recombinant adenoassociated virus vector encoding interleukin-1 receptor antagonist. *Molecular Vision* 2009; 15:1542-1552.
9. Han Z, Boyle DL, Aupperle KR, Bennett B, Manning AM, Firestein GS. Jun N-terminal kinase in rheumatoid arthritis. *J Pharmacol Exp Ther* 1999 Oct; 291(1):124-130.

- 1
2
3 10. Clancy R, Rediske J, Koehne C, Stoyanovsky D, Amin A, Attur M, Iyama K, Abramson
4 SB. Activation of stress-activated protein kinase in osteoarthritic cartilage. Evidence for nitric ox-
5 ide dependence. *Osteoarthritis Cartilage* 2001; 9(4):294-299.
6
7
8 11. Hirt L, Badaut J, Thevenet J, Granziera C, Regli L, Maurer F, Bonny C, Bogousslavsky J. D-
9 JNKII, a Cell-Penetrating c-Jun-N-Terminal Kinase Inhibitor, Protects Against Cell Death in
10 Severe Cerebral Ischemia. *Stroke* 2004; 35:1738-1743.
11
12 12. Touchard E, Omri S, Naud MC, Berdugo M, Deloche C, Abadie C, Jonet L, Jeanny JC,
13 Crisanti P, De Kozak Y, Combette JM, Behar-Cohen F. A peptide inhibitor of c-jun N-terminal
14 kinase for the treatment of endotoxin-induced uveitis. *Invest Ophthalmol Vis Sc* 2010; 51:4683-
15 4693.
16
17 13. Rosenbaum JT, McDevitt HO, Guss RB, Egbert R. Endotoxin-induced uveitis in rats as a
18 model for human disease. *Nature* 1980; 268:611-613.
19
20 14. Hashida M, Fukushima A, Zhang J, Kodama H, Ueno H. Involvement of superoxide generat-
21 ed by polymorphonuclear leukocytes in endotoxin-induced uveitis. *Graefe's Arch Clin Exp Oph-*
22 *thalmol* 2000; 238:359-365.
23
24 15. Behar-Cohen FF, Parel JM, Pouliquen Y, Thillaye-Goldenberg B, Goureau O, Heydolph S,
25 Courtois Y, De Kozak Y. Iontophoresis of dexamethasone in the treatment of endotoxin-induced-
26 uveitis in rats. *Exp Eye Res* 1997; 65(4):533-545.
27
28 16. Ip YT, Davis RJ. Signal transduction by the c-Jun N-terminal kinase (JNK)-from inflammation
29 to development. *Current Opinion in Cell Biology* 1998; 10(2):205-219.
30
31 17. Willaime-Morawek S, Brami-Cherrier K, Mariani J, Caboche J, Brugg B. C-Jun N-terminal
32 kinases/c-Jun and p38 pathways cooperate in ceramide-induced neuronal apoptosis. *Neuroscience*
33 2003; 119(2):387-397.
34
35 18. Chi ZL, Hayasaka S, Zhang XY, Cui HS, Hayasaka Y. A cholinergic agonist attenuates endo-
36 toxin-induced uveitis in rats. *Invest Ophthalmol Vis Sci* 2007; 48(6):2719-2725.
37
38
39
40
41
42
43
44
45
46
47
48
49
50
51
52
53
54
55
56
57
58
59
60

- 1
2
3 19. Reinecke K, Eminel S, Dierck F, Roessner W, Kersting S, Chromik AM, Gavrilova O,
4
5
6 Laukeviciene A, Leuschner I, Waetzig V, Rosenstiel P, Herdegen T, Sina C. The JNK Inhibitor
7
8 XG-102 Protects against TNBS-Induced Colitis. PLoS One 2012 Mar; 7(3):e30985.
9
10 20. Bonny C, Oberson A, Negri S, Sauser C, Schorderet DF. Cell-Permeable Peptide Inhibitors of
11
12 JNK Novel Blockers of β -Cell Death. Diabetes 2001; 50(1):77-82.
13
14 21. El Sanharawi M, Kowalczyk L, Touchard E, Omri S, de Kozak Y, Behar-Cohen F. Protein
15
16 delivery for retinal diseases. From basic considerations to clinical applications. ProgRetin Eye
17
18 Res 2010 Nov; 29(6):443-465.
19
20 22. Weijtens O, Feron EJ, Schoemaker RC, Cohen AF, Lentjes EG, Romijn FP, van Meurs JC.
21
22 High concentration of dexamethasone in aqueous and vitreous after subconjunctival injection.
23
24 Am J Ophthalmol 1999; 128(2):192-197.
25
26 23. Weijtens O, Schoemaker RC, Cohen AF, Romijn FP, Lentjes EG, van Rooij J, van Meurs
27
28 JC. Dexamethasone concentration in vitreous and serum after oral administration. Am J Ophthal-
29
30 mol 1998; 125(5):673-679.
31
32 24. Weijtens O, van der Sluijs FA, Schoemaker RC, Lentjes EG, Cohen AF, Romijn FP, van
33
34 Meurs JC. Peribulbar corticosteroid injection. Vitreal and serum concentrations after dexame-
35
36 thasone disodium phosphate injection. Am J Ophthalmol 1997 Mar; 123(3):358-363.
37
38
39
40
41
42
43
44
45
46
47
48
49
50
51
52
53
54
55
56
57
58
59
60

Legends

Figure 1: Clinical evaluation of XG-102 efficacy in Endotoxin-Induced Uveitis.

Clinical scores (mean \pm SEM arbitrary units, a.u.) were evaluated at the peak of the disease, 24 hours after intravenous (**IV, A**; $n \geq 8$ eyes per group), intravitreal (**IVT, B**; $n \geq 4$ eyes per group) and sub-conjunctival (**SCJ, C**; $n \geq 5$ eyes per group) injections of different doses of XG-102. Dexamethasone phosphate IV ($n=6$), IVT ($n=5$) or SCJ ($n=5$) injections were used as positive control. Comparisons were respectively made with vehicle IV ($n=8$), IVT ($n=12$) or SCJ ($n=6$) injections. Clinical signs of uveitis were significantly reduced after: (**A**) IV injections of 35 μg (*) and 355 μg (***) of XG-102; (**B**) IVT injections of 0.08 (**), 0.2 (**) and 2.2 μg (**) of XG-102; (**C**) SCJ injections of 1.8 μg (*) and 22 μg (**) of XG-102. No statistical difference (**ns**) was observed between the clinical scores of the IV-injected 355 μg , the SCJ-injected 22 μg and all the IVT-injected doses and those of the Dexamethasone phosphate groups for the respective routes of administration. * $P < 0.05$, ** $p < 0.01$, *** $p < 0.001$.

Figure 2: Analysis of c-Jun phosphorylation in “RPE-choroid-sclera” complex.

Western blots were performed 24 hours after intravenous (**IV** of 35 μg , **A**), intravitreal (**IVT** of 0.2 μg , **B**) and sub-conjunctival (**SCJ** of 1.8 μg , **C**) injections of XG-102, and compared to the vehicle-injected eyes ($n=2$ pooled “RPE-choroid-sclera” complex per group). The **immunoblots** (*top*) of Phospho c-Jun [Ser 63] and of the α -tubulin reporter protein, and their quantization by **densitometry** (*bottom*) demonstrated that the phosphorylation of c-Jun was strongly reduced by XG-102 delivered by the three routes of administration.

1
2
3 **Figure 3: Effect of XG-102 on PMN cells infiltration in ocular tissues.**
4
5

6 Polymorphonuclear (PMN) leukocytes infiltration was evaluated 24 hours after EIU induction in
7 eyes treated with 35 μg -XG-102 **IV (A)**, 0.2 μg -XG-102 **IVT (B)** and 1.8 μg -XG-102 **SCJ (C)**
8 injections on frozen sections (3 eyes per group, 3 sections per eye).
9
10

11
12
13
14
15
16
17 **Figure 4: Effect of XG-102 on iNOS expression in neuroretinal cells.**
18

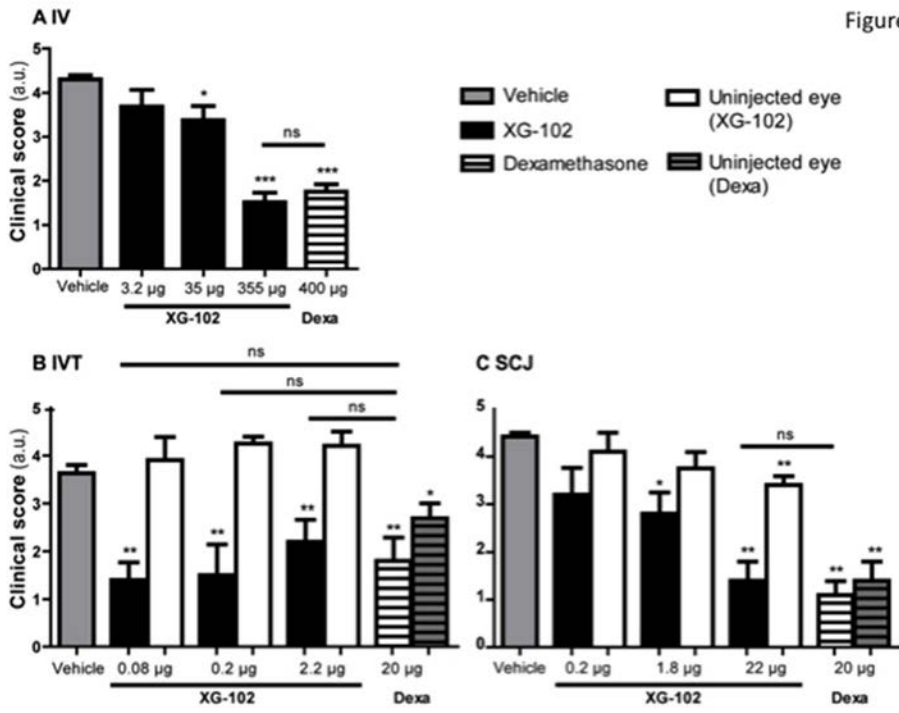
19 Mean \pm SEM relative band intensity were determined after the detection of iNOS expression in
20 retinal cells of the eyes treated with 3.2 μg and 35 μg of XG-102 **IV (A, n \geq 3)**, 0.2 μg and 2.2 μg
21 of XG-102 **IVT (B, n \geq 2)** and 1.8 μg XG-102 **SCJ (C, n=3)** injections and compared with those of
22 the control vehicle-injected eyes, 24 hours after EIU induction. Representative RT PCR products
23 visualized by ethidium bromide staining are shown in the *bottom plan*. *P<0.05.
24
25
26
27
28
29
30

31
32
33
34 **Figure 5: Effect of XG-102 on CINC-1 expression in neuroretinal cells.**
35

36 Mean \pm SEM relative band intensity were determined after the detection of CINC-1 expression in
37 retinal cells of the eyes treated with 35 μg of XG-102 **IV (A, n \geq 2)**, 0.2 μg of XG-102 **IVT (B,**
38 **n \geq 3)** and 1.8 μg -XG-102 **SCJ injection (n \geq 3)** and compared with that of vehicle control eyes, 24
39 hours after EIU induction. Representative RT PCR products visualized by ethidium bromide
40 staining are shown in the *bottom plan*.
41
42
43
44
45
46
47
48
49
50
51
52
53
54
55
56
57
58
59
60

1
2
3
4
5
6
7
8
9
10
11
12
13
14
15
16
17
18
19
20
21
22
23
24
25
26
27
28
29
30
31
32
33
34
35
36
37
38
39
40
41
42
43
44
45
46
47
48
49
50
51
52
53
54
55
56
57
58
59
60

Figure 1



211x158mm (72 x 72 DPI)

1
2
3
4
5
6
7
8
9
10
11
12
13
14
15
16
17
18
19
20
21
22
23
24
25
26
27
28
29
30
31
32
33
34
35
36
37
38
39
40
41
42
43
44
45
46
47
48
49
50
51
52
53
54
55
56
57
58
59
60

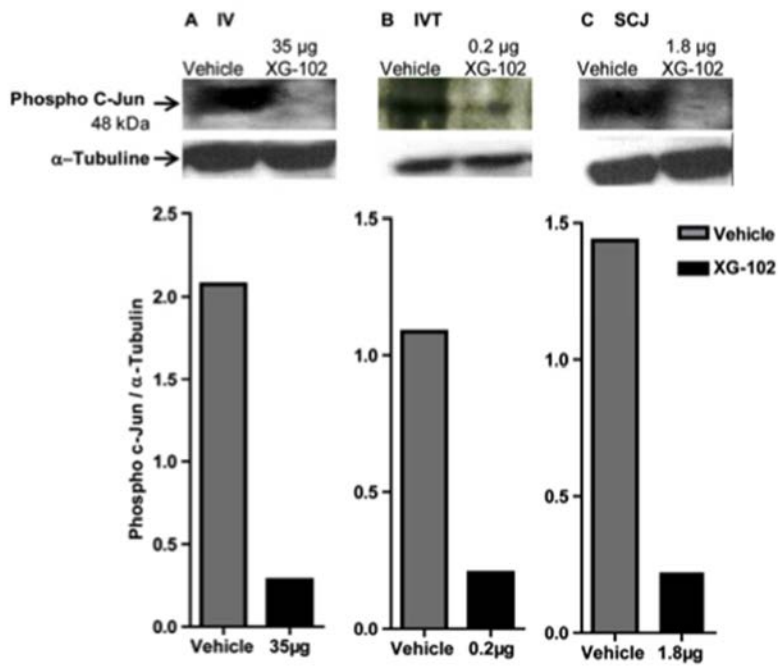


Figure 2

211x158mm (72 x 72 DPI)

1
2
3
4
5
6
7
8
9
10
11
12
13
14
15
16
17
18
19
20
21
22
23
24
25
26
27
28
29
30
31
32
33
34
35
36
37
38
39
40
41
42
43
44
45
46
47
48
49
50
51
52
53
54
55
56
57
58
59
60

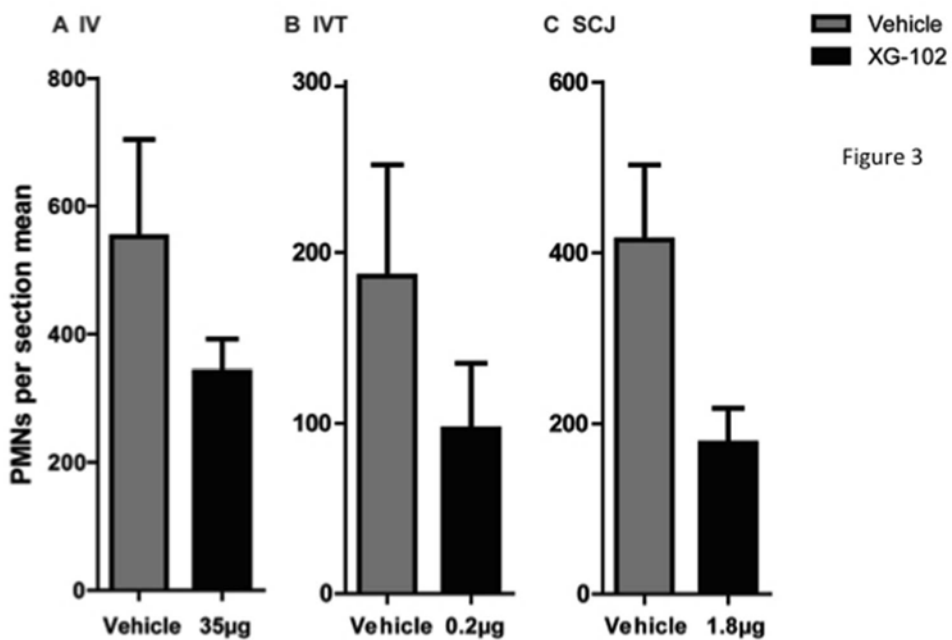
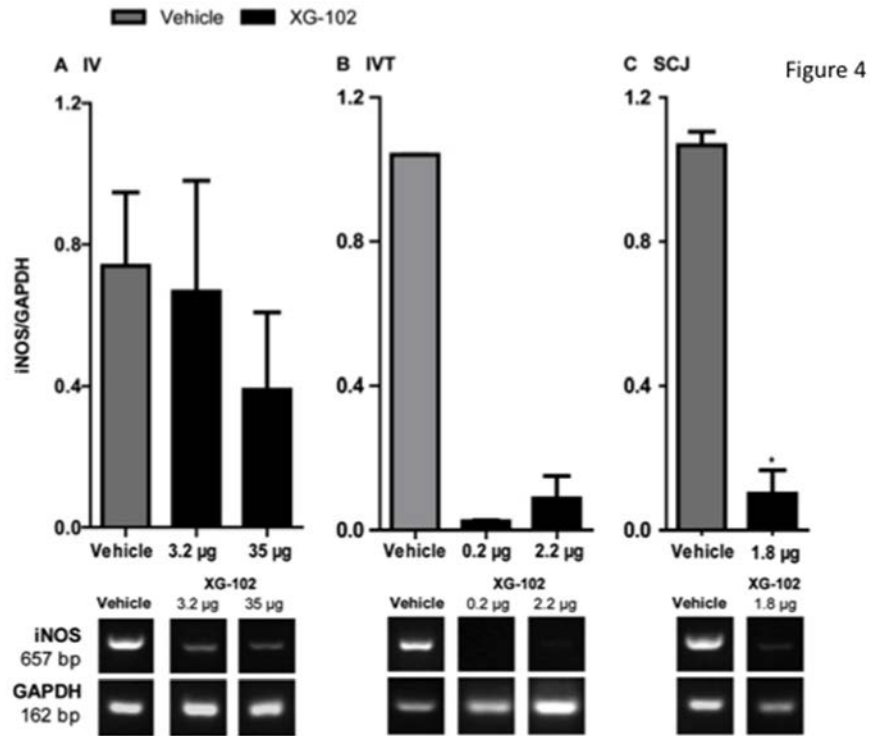


Figure 3

211x158mm (72 x 72 DPI)



211x158mm (72 x 72 DPI)

1
2
3
4
5
6
7
8
9
10
11
12
13
14
15
16
17
18
19
20
21
22
23
24
25
26
27
28
29
30
31
32
33
34
35
36
37
38
39
40
41
42
43
44
45
46
47
48
49
50
51
52
53
54
55
56
57
58
59
60

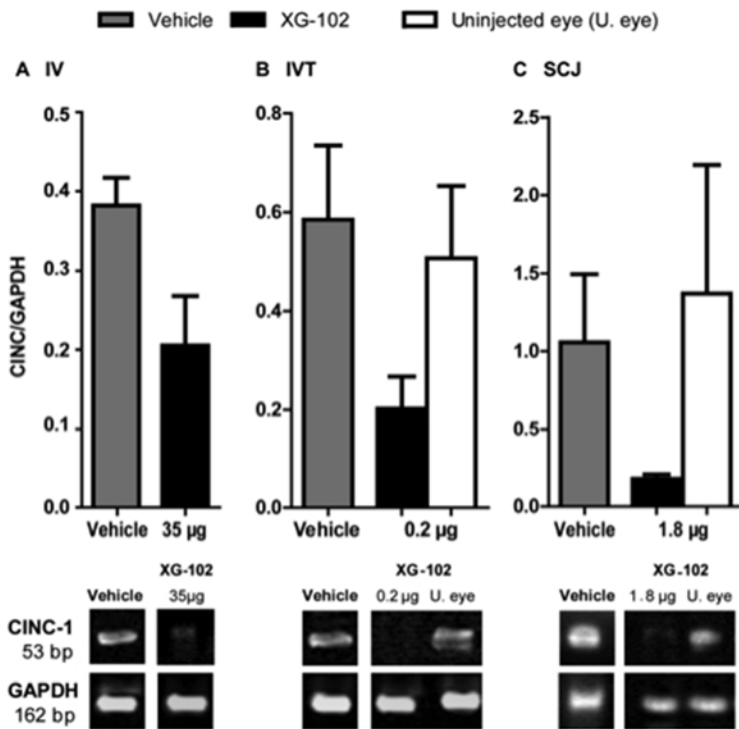


Figure 5

211x158mm (72 x 72 DPI)